Electronic Supplementary Material (ESI) for RSC Sustainability.

Exploration of Bis(pentafluorophenyl)borinic Acid as an Electronically Saturated, Bench-top Stable Lewis Acid Catalyst

Electronic Supplementary Information

Taylor P. L. Cosby, Christopher B. Caputo

Department of Chemistry
York University
158 Campus Walk, North York, ON CA
caputo@yorku.ca

Table of Contents

General Considerations

Reactions were carried out both under atmospheric and air-free conditions. Some reactions were carried out under an atmosphere of anhydrous N_2 using standard glovebox (MBraun LABstar) and/or Schlenk techniques unless otherwise stated. All glassware, needles, and stir bars were dried in an oven at 140 °C and/or flame dried under vacuum before use. All solvents were obtained from an MBraun MB-SPS 800 solvent purification system, collected under vacuum, and dried over 4Å molecular sieves prior to use. All commercially available reagents were used as received from Sigma Aldrich, TCI Chemicals, or Oakwood Chemicals and used without further purification. Tris(pentafluorophenyl)borane ($B(C_6F_5)_3$)[1] and bis(pentafluorophenyl)borane[1] were synthesized following known literature procedures. Deuterated solvents were degassed by employing a freeze-pump-thaw procedure and dried over 4Å molecular sieves before use. Nuclear magnetic resonance (NMR) spectra were acquired on either Bruker NEO 700 MHz, DRX 600 MHz, Bruker ARX 400 MHz, or Bruker ARX 300 MHz NMR spectrometers at 25 °C and referenced to the corresponding residual solvent peak of deuterated solvent (benzene-d_8, dichloromethane-d_2, chloroform-d, acetonitrile-d_3). Chemical shifts for protons (^{1}H) and carbons (^{13}C) are reported relative to tetramethylsilane ($SiMe_4$) and were referenced to residual protiated or carbon solvent peaks. Chemical shifts for fluorine (^{19}F) and boron (^{11}B) are reported relative to 15 % BF_3-Et_2O and chemical shifts for nitrogen (^{15}N) are reported relative to ammonia (NH_3) and referenced to nitromethane. NMR spectra were collected using Topspin 4.0.1 software and analyzed using Mestrenova 14.3.1 software. Chemical shifts are reported in ppm, coupling constants reported in hertz (Hz), and conventional abbreviations for multiplicity were used (br = broad, s = singlet, d = doublet, t = triplet, dt = doublet of triplets, m = multiplet). Inversion recovery experiments were performed on all catalytic substrates and the appropriate relaxation delay values were applied when collecting NMR spectra. All percent conversions in catalytic reactions were calculated using NMR integration in reference to an internal standard (mesitylene, C_9H_{12}). Mass spectrometry data was provided from the AIMS Mass Spectrometry Laboratory at the University of Toronto and was acquired using dual electrospray ionization in positive mode on an Agilent 6538 UHD instrument.

Synthetic Procedures and Characterization

9-(bis(perfluorophenyl)boraneyl)-9H-carbazole (**1**)[2]:

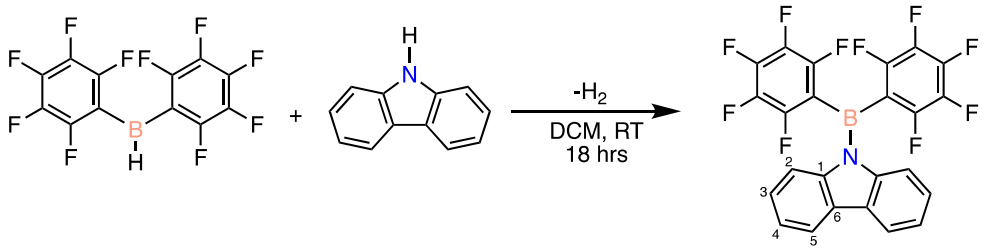

As previously reported, a solution of carbazole (0.048 g, 0.289 mmol, 1eq.) was prepared in approximately 3 mL of DCM. A second solution of bis(pentafluorophenyl)borane (0.100 g, 0.289 mmol, 1eq.) was prepared in approximately 3 mL of DCM. The carbazole solution was added dropwise while stirring to the bis(pentafluorophenyl)borane solution and allowed to stir overnight with a loosened vial cap, resulting in a bright yellow solution. The solvent was removed *in vacuo* resulting in a pale-yellow precipitate. The solid was triturated 3 times with 5 mL of pentanes. Multinuclear NMR analysis aligned with previously reported data of the synthesis of **1**. Yield = 0.106 g, 73 %.

^{1}H NMR (400 MHz, C_6D_6) δ: 7.57 (d, 2H, *J* = 8.0 Hz), 7.05 (t, 2H, *J* = 8.0 Hz), 6.98 (d, 2H, *J* = 8.0 Hz), 6.92 (m, 2H).

^{13}C{^{1}H} NMR (176 MHz, C_6D_6) δ: 146.7 (m, *o*-CF, *J* = 246.4 Hz), 143.4 (m, *p*-CF, *J* = 257.0 Hz), 143.4 (s, C_1), 138.1 (m, *m*-CF, *J* = 255.2 Hz), 129.8 (s, C_6), 127.6 (s, C_3), 125. 7 (s, C_4), 120.7 (s, C_2), 115.3 (s, C_5), 112.3 (br, *ipso*-C).

^{19}F NMR (376 MHz, C_6D_6) δ: -131.4 (m, 4F, *o*-F), -147.9 (t, 2F, *p*-F, J = 22.6 Hz), -159.3 (m, 4F, *m*-F).

^{11}B{^{1}H} NMR (128 MHz, C_6D_6) δ: 40.6 (br).

^{15}N NMR (71 MHz, C_6D_6) δ: 169.1 (s).

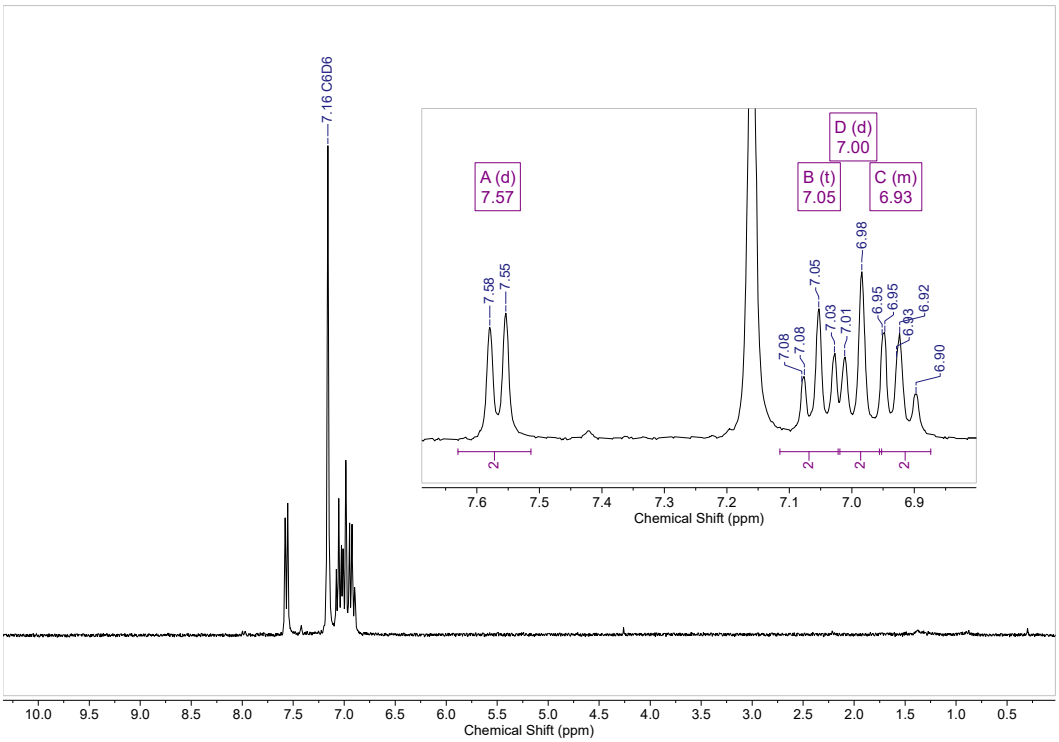

Fig. S1: ^{1}H NMR spectrum of aminoborane **1** in C_6D_6.

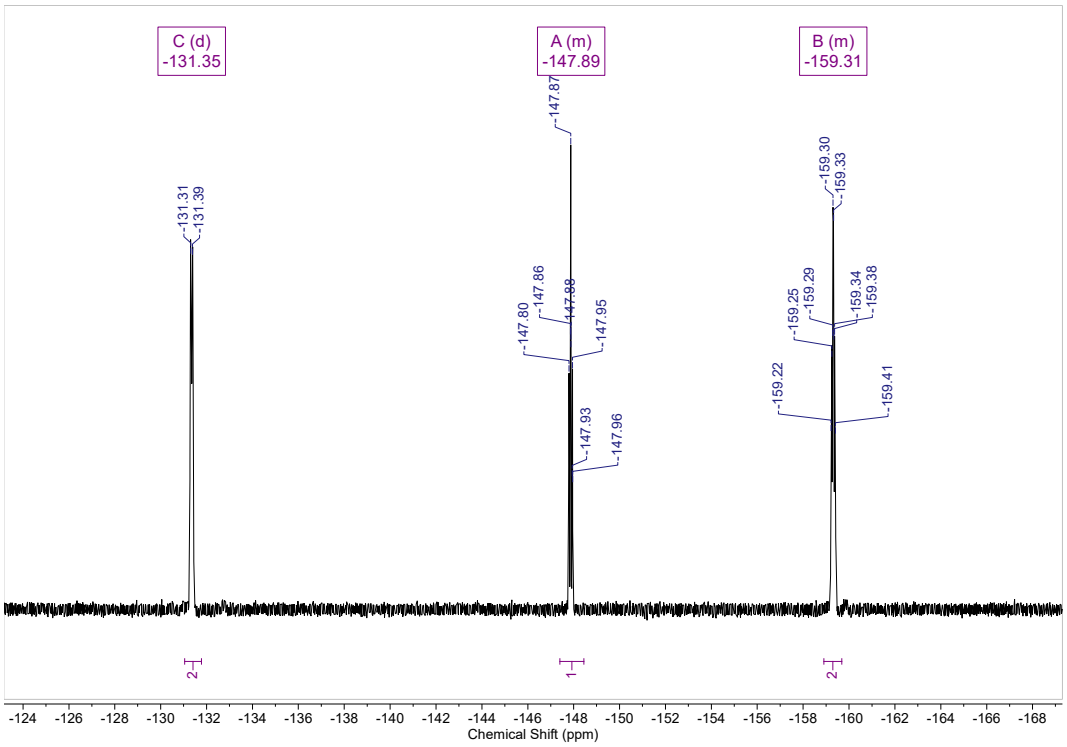

Fig. S2: ^{19}F NMR spectrum of aminoborane **1** in C_6D_6.

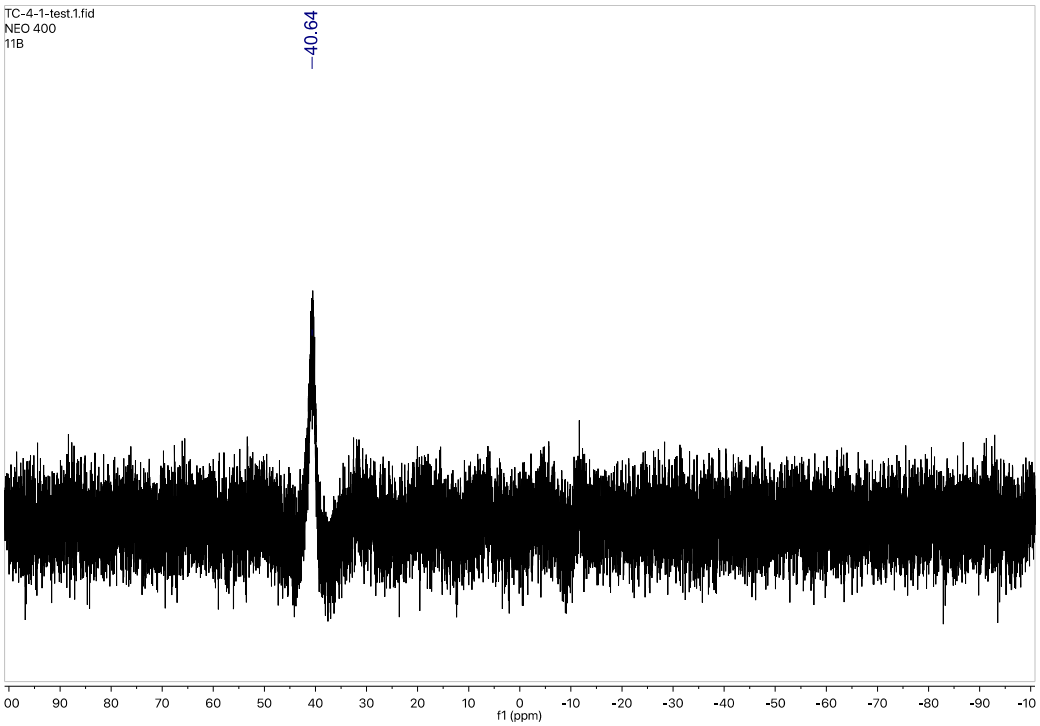

Fig. S3: $^{11}B\{^1H\}$ NMR spectrum of aminoborane **1** in C_6D_6.

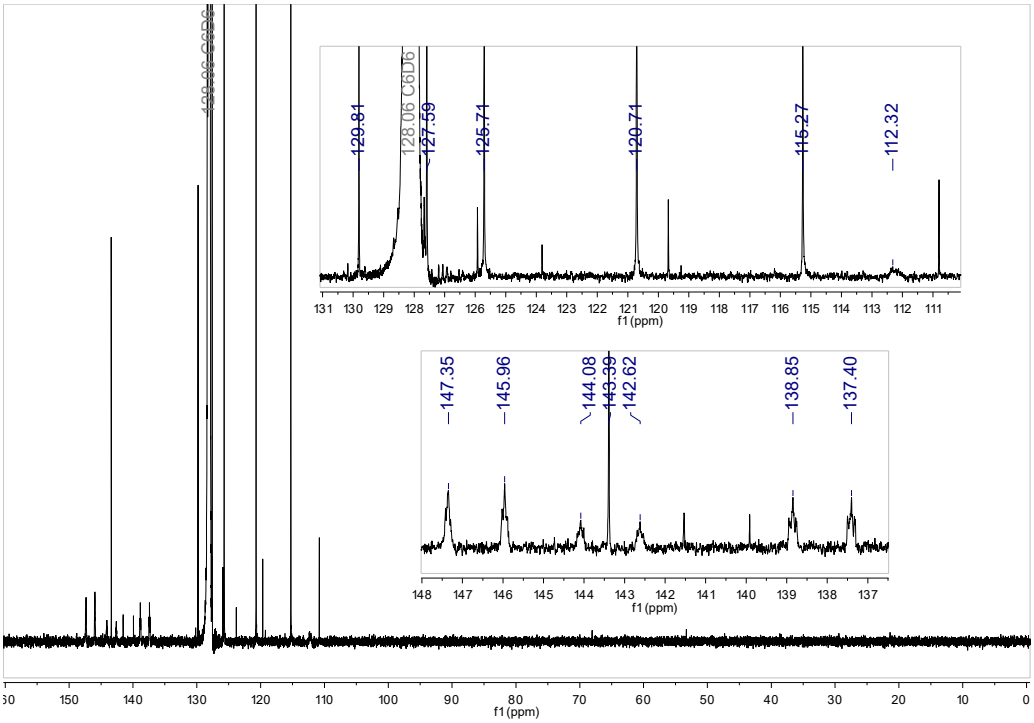

Fig. S4: $^{13}C\{^1H\}$ NMR spectrum of aminoborane **1** in C_6D_6.

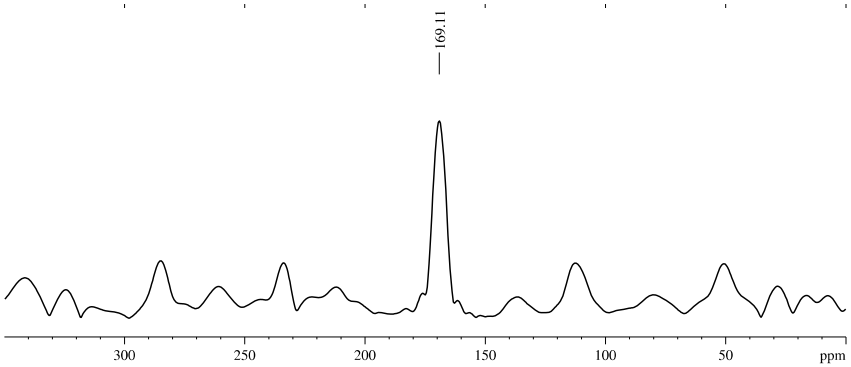

Fig. S5: ^{15}N NMR spectrum of aminoborane **1** in C_6D_6.

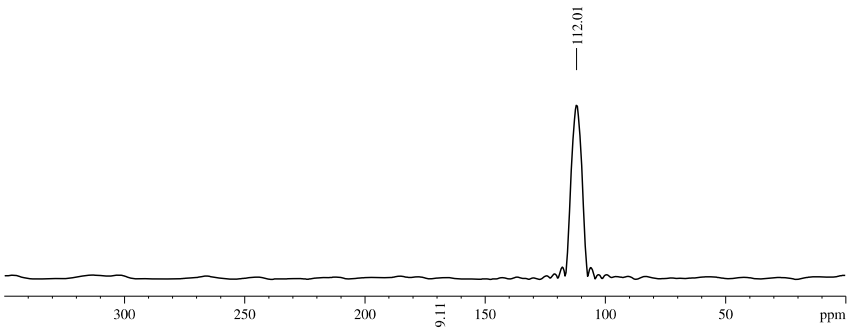

Fig. S6: ^{15}N NMR

Bis(pentafluorophenyl)borinic acid (**2**):

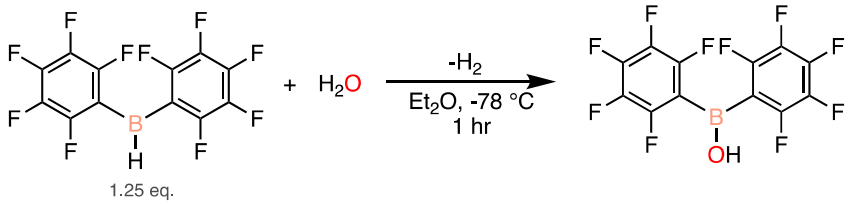

Piers' borane (0.100 g, 0.289 mmol, 1.25 eq.) was dissolved in approximately 4 mL of anhydrous diethyl ether (Et_2O) and cooled to -78 °C in a dry ice/acetone bath. A solution of water in Et_2O with a concentration of 0.2 M was prepared and the appropriate volume (2.0 mL) was added dropwise to the solution of Piers' borane. The solution was stirred for 1 hour at -78 °C and volatiles were removed *in vacuo* to yield a colourless oil which was solidified upon evaporation of pentanes. The product was obtained following trituration of the white solid with hexanes. Multinuclear NMR analysis aligned with previously reported data of the synthesis of bis(pentafluorophenyl)borinic acid.[3] Yield = 0.084, 80 %.

^{1}H NMR (400 MHz, $CDCl_3$) δ: 7.23 (br, 1H).

^{13}C{^{1}H} NMR (176 MHz, $CDCl_3$) δ: 148.9 (m, *o*-CF, *J* = 249.6 Hz)), 143.8 (m, *p*-CF, *J* = 259.3 Hz), 137.6 (m, *m*-CF, *J* = 253.5 Hz), 108.7 (br, *ipso*-C).

^{19}F NMR (376 MHz, $CDCl_3$) δ: -132.4 (m, 4F, *o*-F), -147.2 (t, 2F, *p*-F, *J* = 21.0 Hz), -160.5 (m, 4F, *m*-F).

^{11}B{^{1}H} NMR (128 MHz, $CDCl_3$) δ: 40.8 (br).

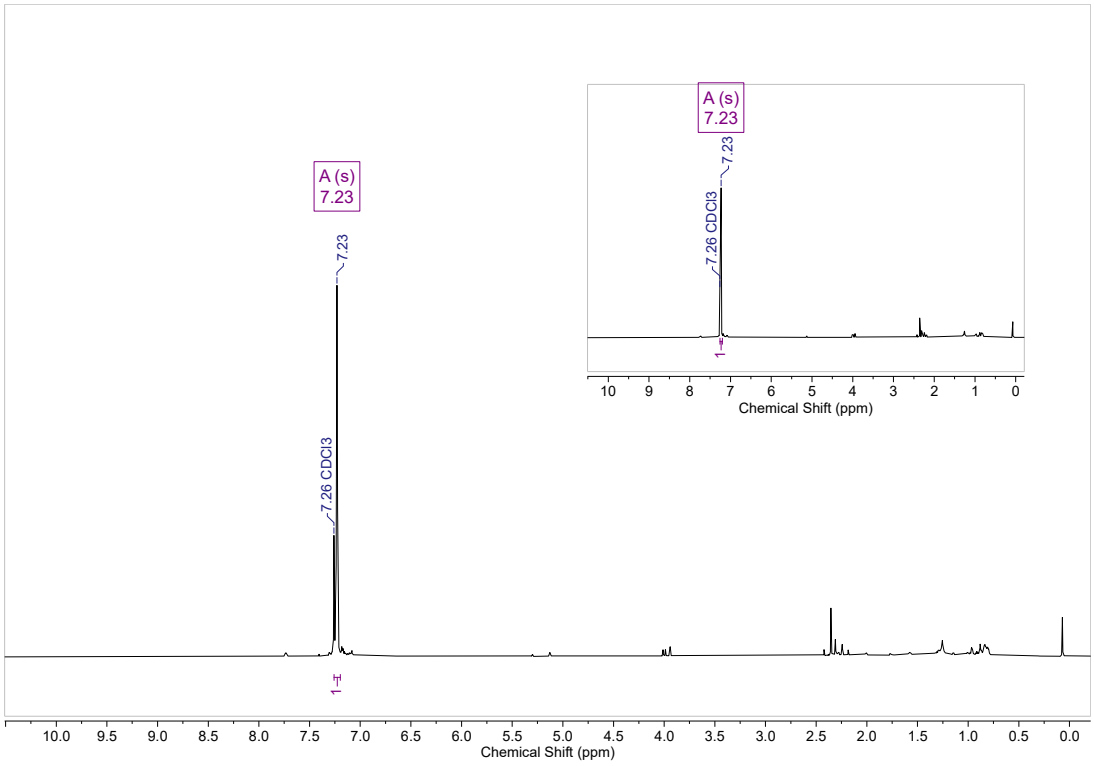

Fig. S7: ^{1}H NMR spectrum of borinic acid **2** in $CDCl_3$.

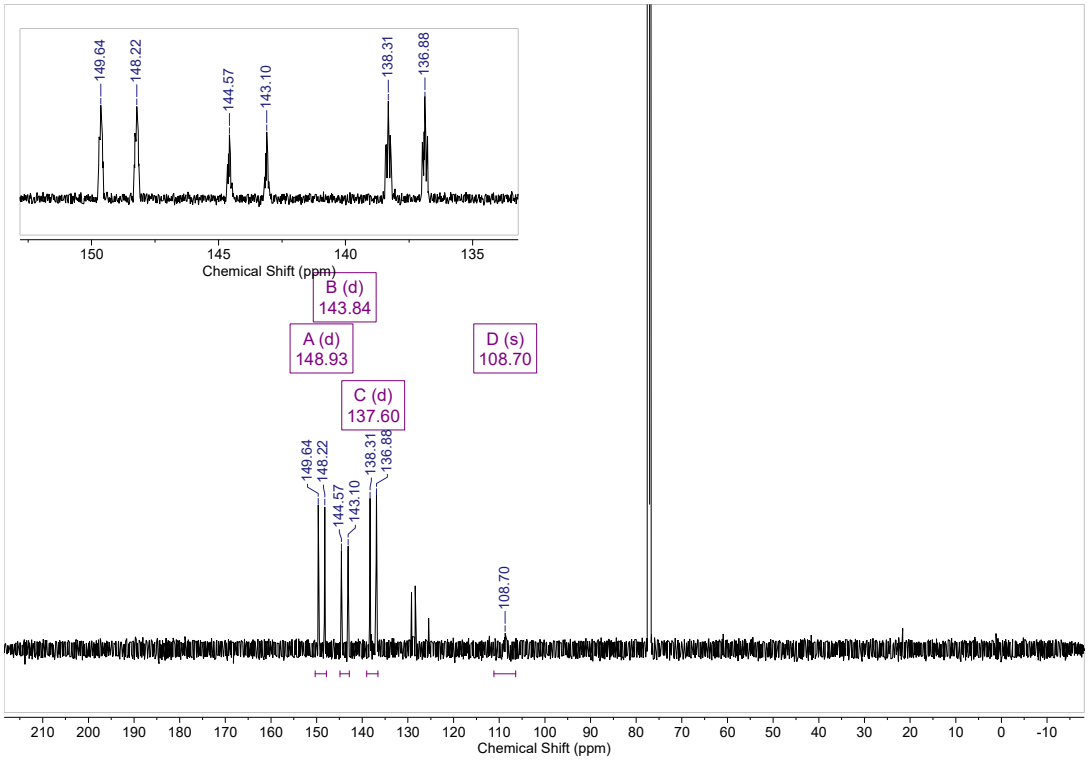

Fig. S8: $^{13}C\{^{1}H\}$ NMR spectrum of borinic acid **2** in $CDCl_3$.

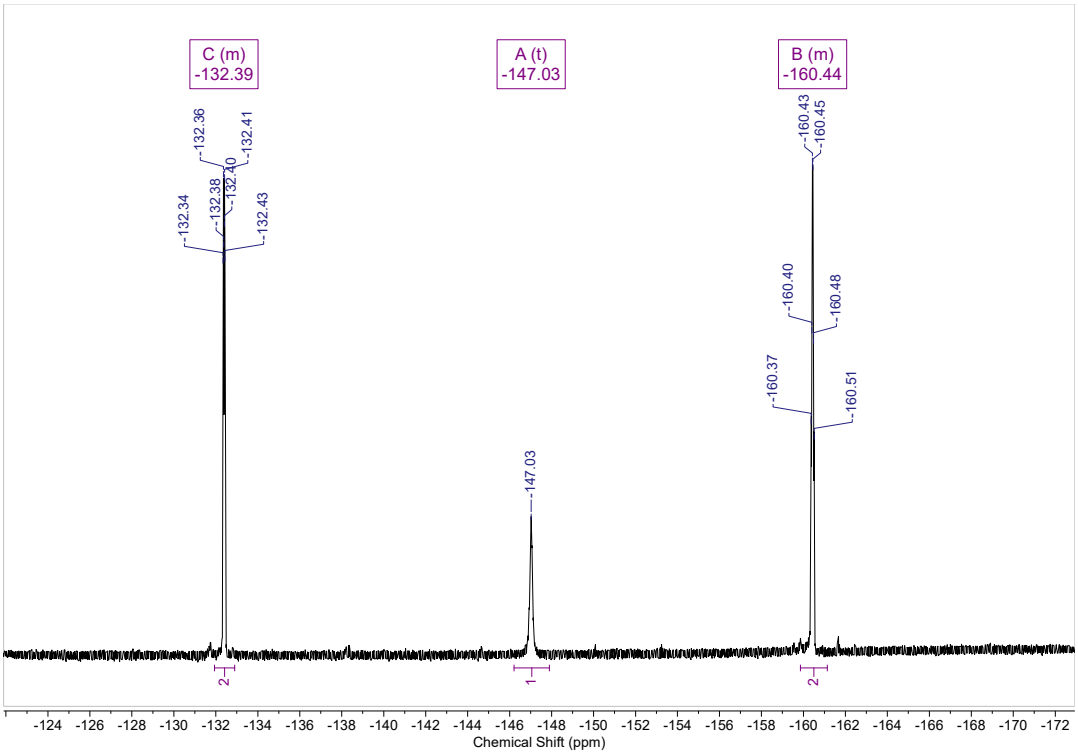

Fig. S9: ^{19}F NMR spectrum of borinic acid **2** in $CDCl_3$.

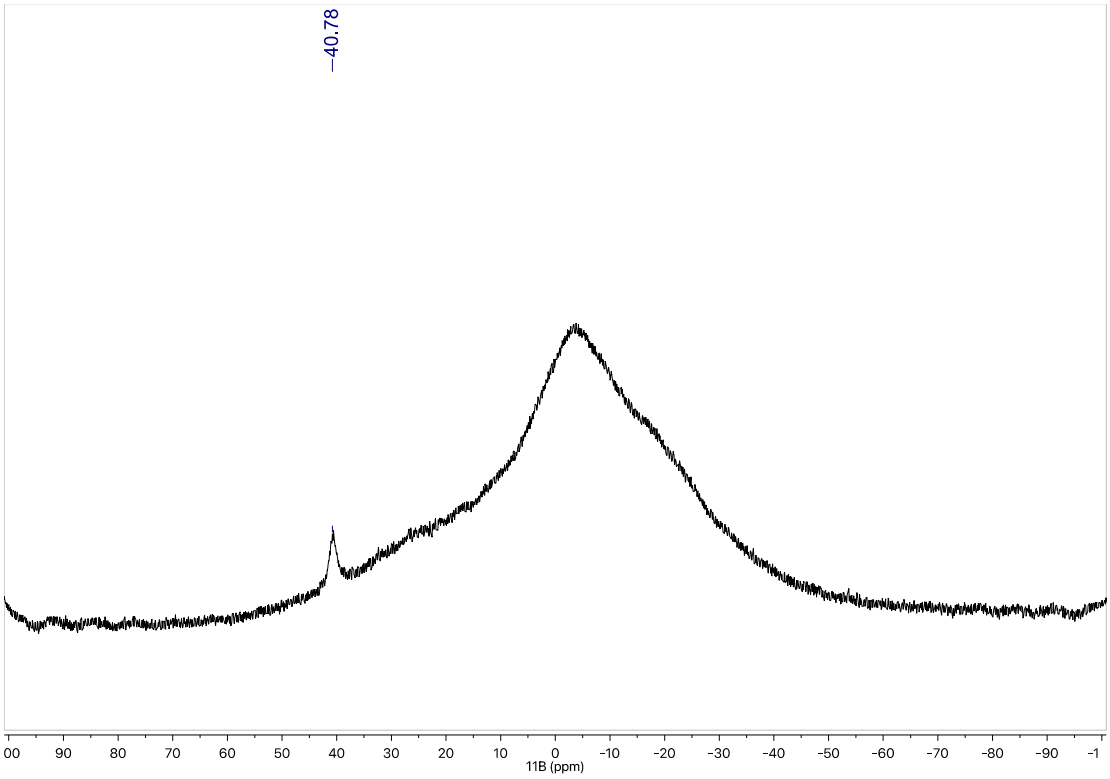

Fig. S10: $^{11}B\{^1H\}$ NMR spectrum of borinic acid **2** in $CDCl_3$.

Assessment of Lewis Acidity

General procedure for Gutmann-Beckett tests: Triethylphosphine oxide (TEPO) (0.0027 g, 0.020 mmol, 1 eq.) and **1**, **2**, or **3** (0.020 mmol, 1 eq.) were dissolved in CD_2Cl_2 in a J-Young NMR tube. The NMR tube was sealed and $^{31}P\{^1H\}$ NMR spectra were recorded. The acceptor number (AN) was calculated using the following formula: $AN = 2.21(\delta_{sample} - \delta_{TEPO,DCM})$.[4]

Table S1: Gutmann-Beckett analysis of compounds **1** and **2** using stoichiometric amounts of TEPO, including $^{31}P\{^1H\}$ chemical shifts and acceptor numbers

Compound	$^{31}P\{^1H\}$ Chemical Shift	Acceptor Number (AN)
1	77.0	59
2	75.2	55

NMR spectra of Gutmann-Beckett tests with 1 and 2

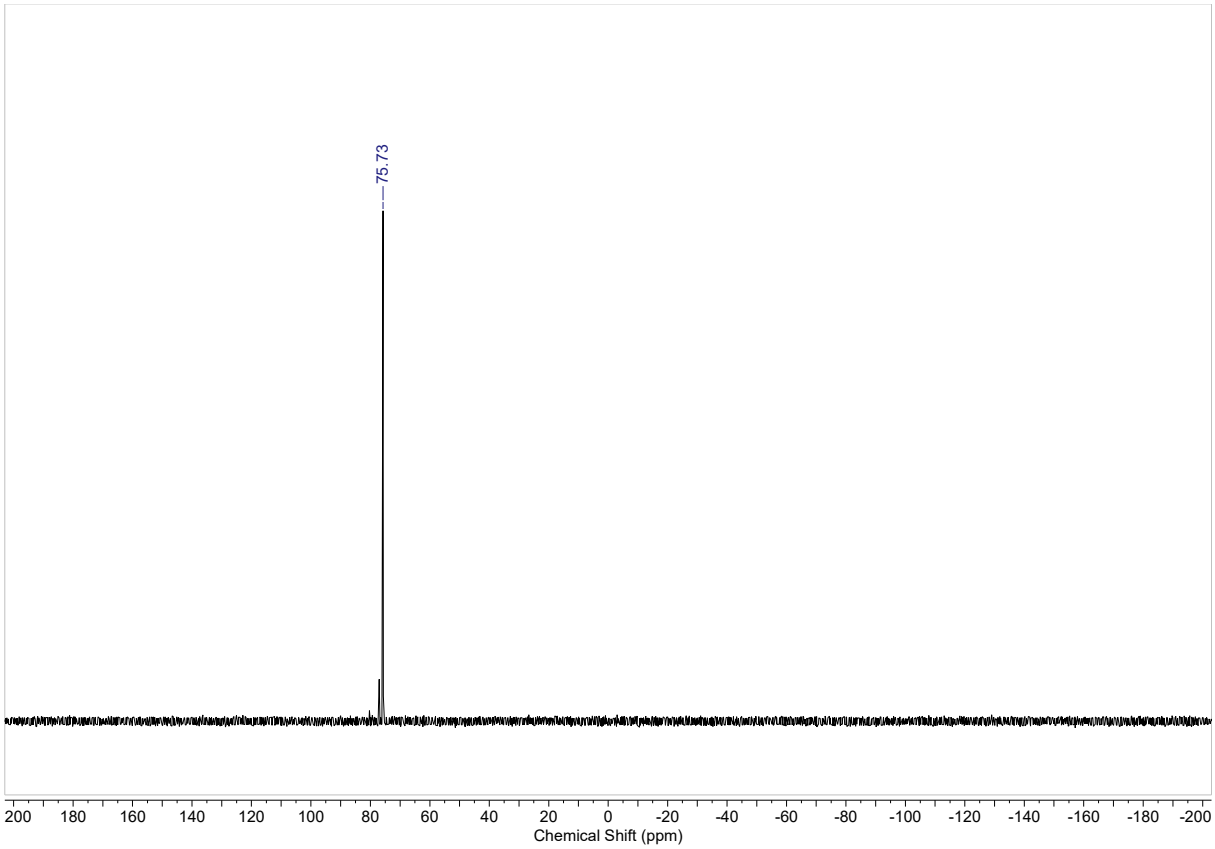

Fig S11: $^{31}P\{^1H\}$ NMR spectrum of equimolar triethylphosphine oxide and **1**.

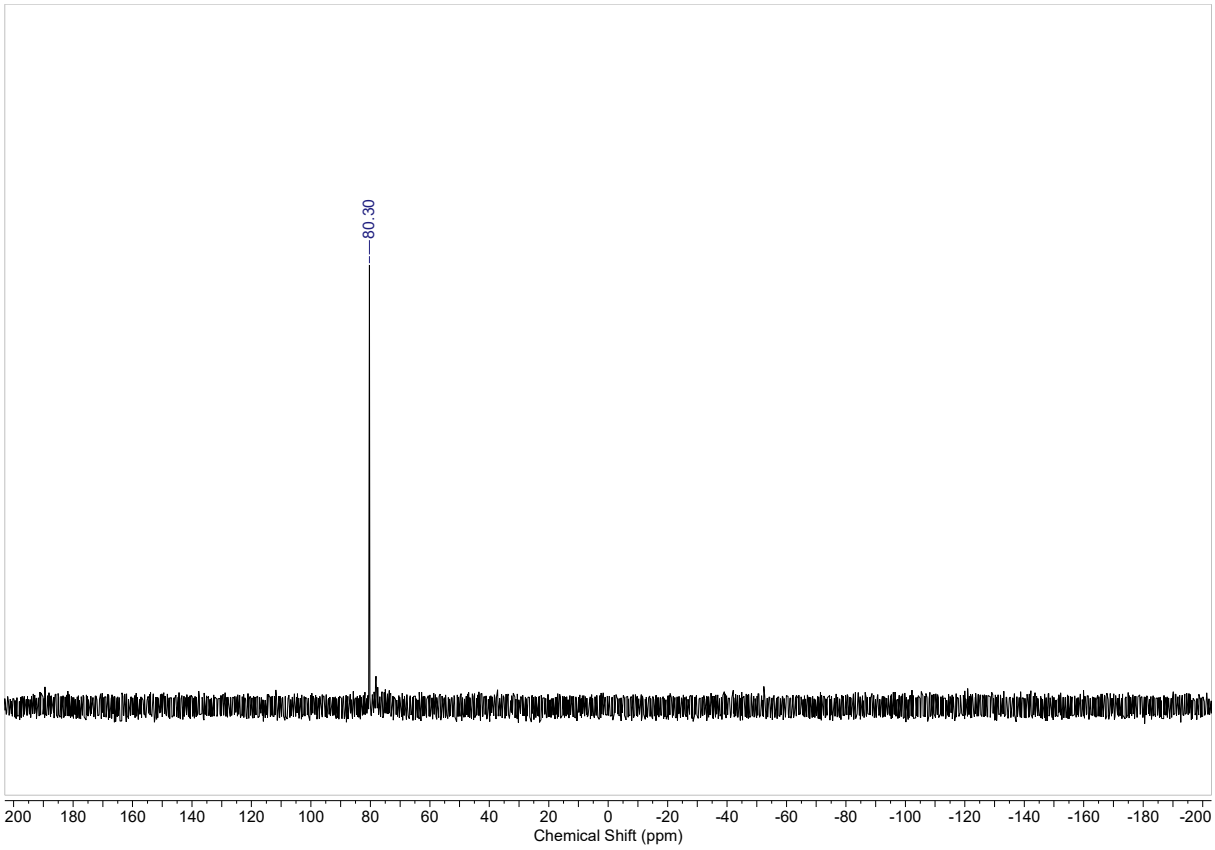

Fig S12: $^{31}P\{^{1}H\}$ NMR spectrum of equimolar triethylphosphine oxide and **2**.

Stability Study of 1 and 2

Solution Stability Assessment

1, **2** or $B(C_6F_5)_3$ (0.029 mmol) were dissolved in 0.6 mL dry benzene-d_6 or $CDCl_3$ in a J-Young NMR tube inside the glovebox. The NMR tube was brought outside the glovebox and the J-Young screw cap was loosened, exposing the solution to ambient atmosphere. The decomposition was monitored over time by acquiring ^1H and $^{19}F\{^1H\}$ NMR spectra. In the case of **2** and $B(C_6F_5)_3$, only $^{19}F\{^1H\}$ NMR spectroscopy was used as the signals in the ^1H NMR were not very diagnostic.

Aminoborane 1:

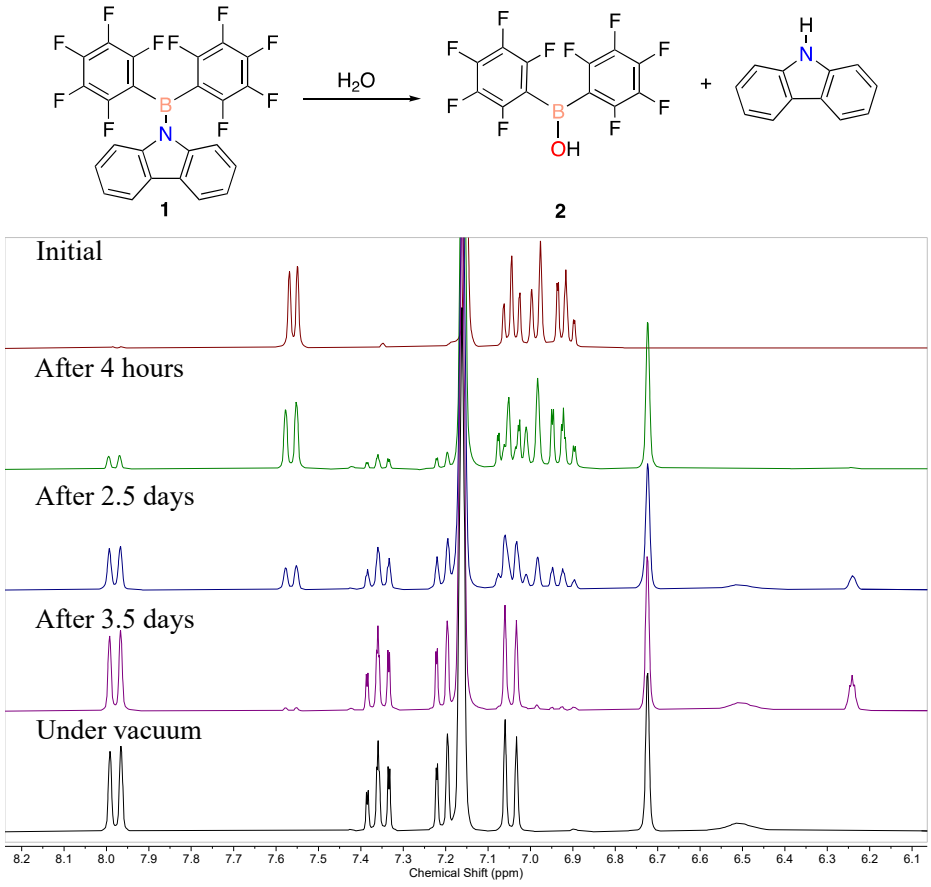

Fig. S13: Stacked ^1H NMR spectra of aminoborane **1** in solution upon exposure to atmosphere in C_6D_6.

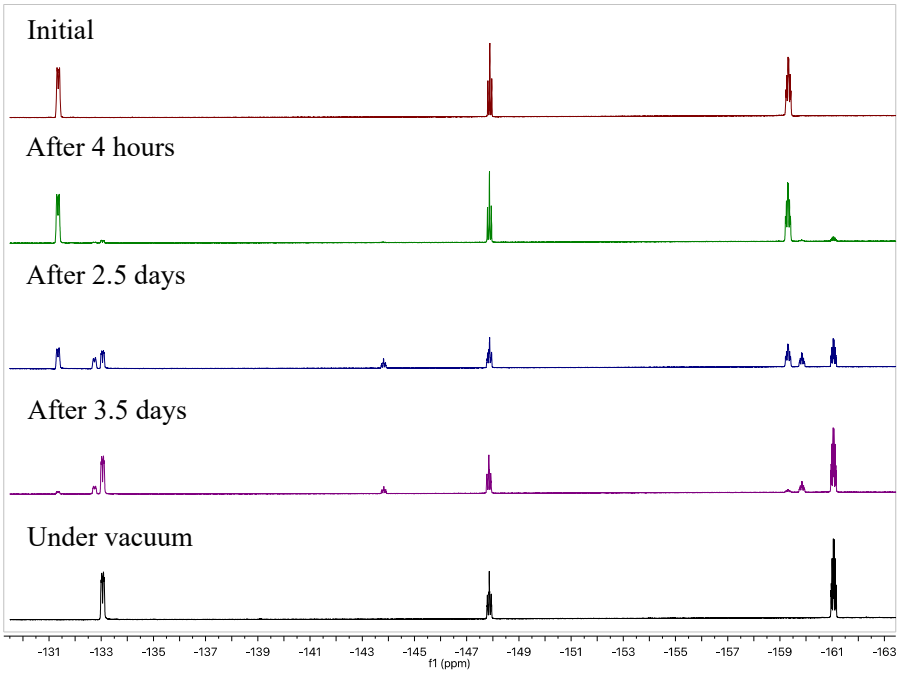

Fig. S14: Stacked $^{19}F\{^{1}H\}$ NMR spectra of aminoborane **1** in solution upon exposure to atmosphere in C_6D_6.

Borinic acid 2:

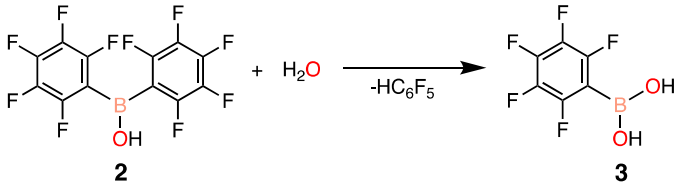

2 **3**

***Note**: Pentafluorophenylboronic acid was tested independently for catalytic activity and was not found to be effective in the hydrosilylation of carbonyls.*

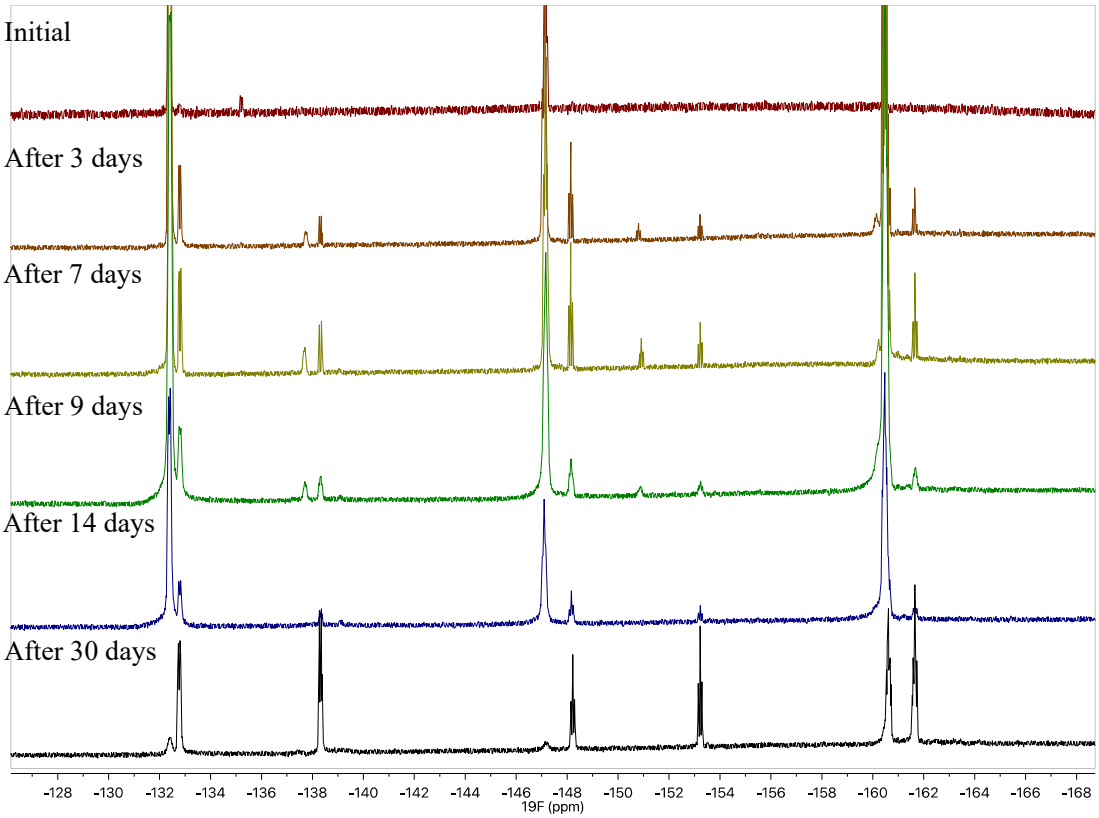

***Fig S15**:* Stacked $^{19}F\{^{1}H\}$ NMR spectra of borinic acid **2** in solution upon exposure to atmosphere in $CDCl_3$.

Tris(pentafluorophenyl)borane ($B(C_6F_5)_3$):

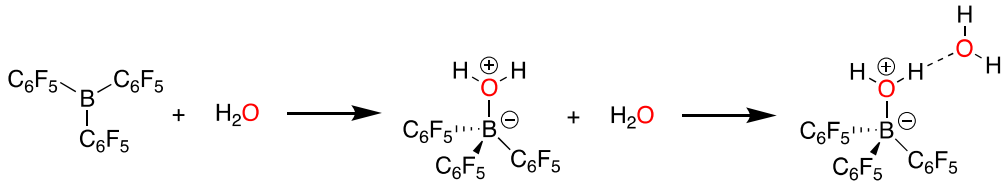

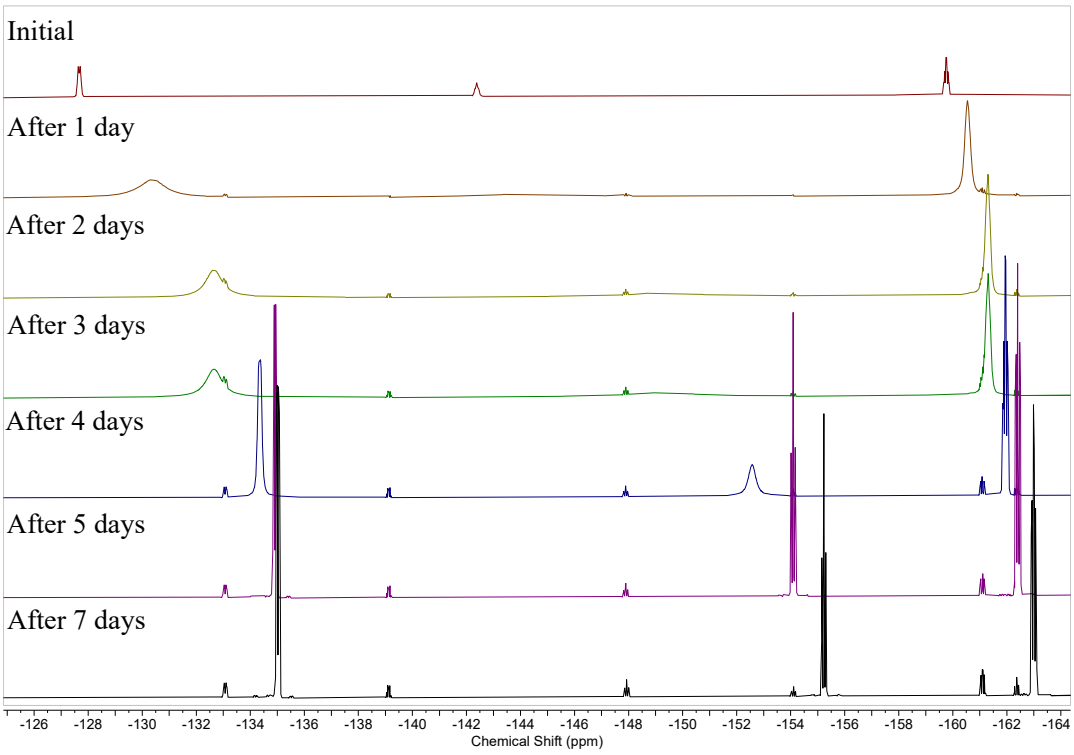

***Fig S16**:* Stacked $^{19}F\{^{1}H\}$ NMR spectra of $B(C_6F_5)_3$ in solution upon exposure to atmosphere in C_6D_6.

Solid State Stability Assessment

To scintillation vials, approximately 50 mg of **1**, **2** or $B(C_6F_5)_3$were added separately inside the glovebox. Each vial was suited with a bleed needle and brought out of the glovebox, exposing them to ambient atmosphere. Each of the boranes were monitored for decomposition over time by dissolving approximately 5 mg of solid at various time points in 0.5 mL of benzene-d_6 or $CDCl_3$ and acquiring ^1H and $^{19}F\{^1H\}$ NMR spectra. In the case of **2** and $B(C_6F_5)_3$, only $^{19}F\{^1H\}$ NMR spectroscopy was used as the signals in the ^1H NMR were not very diagnostic.

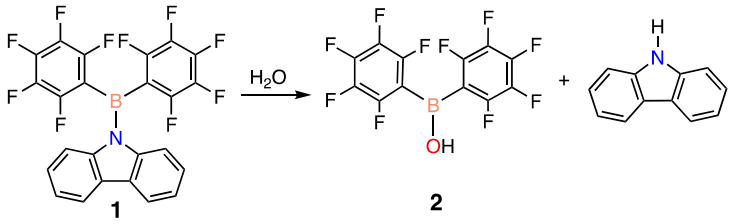

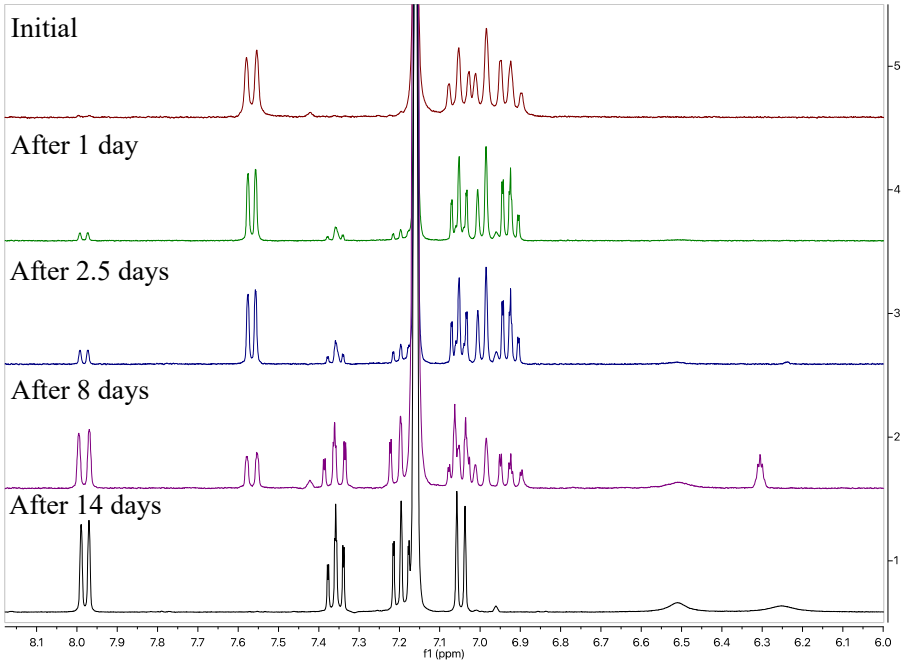

***Fig. S17**:* Stacked ^1H NMR spectra of aminoborane **1** in the solid state upon exposure to atmosphere in C_6D_6.

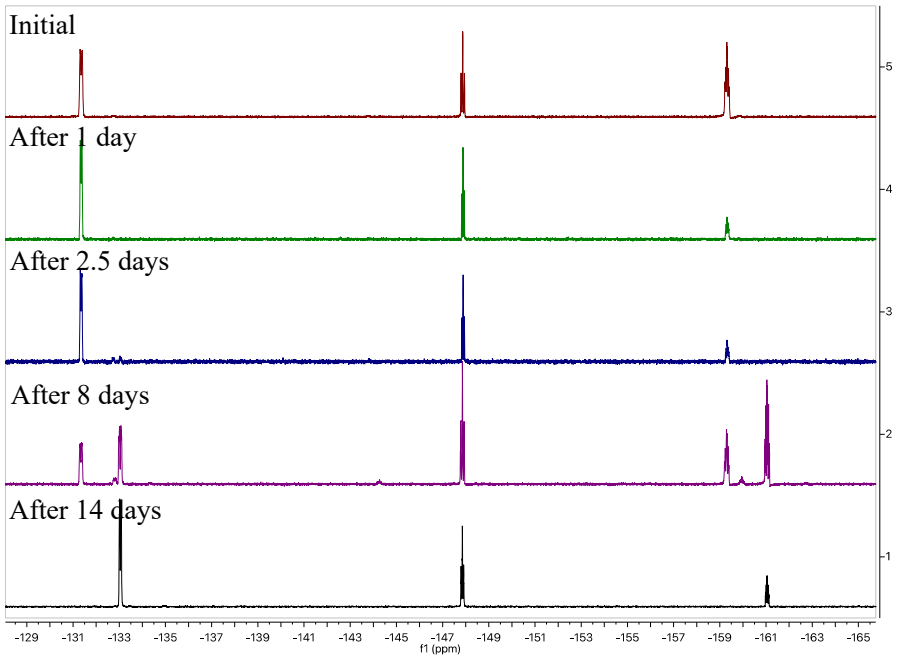

Fig. S18: Stacked $^{19}F\{^{1}H\}$ NMR spectra of aminoborane **1** in the solid state upon exposure to atmosphere in C_6D_6.

Borinic acid 2:

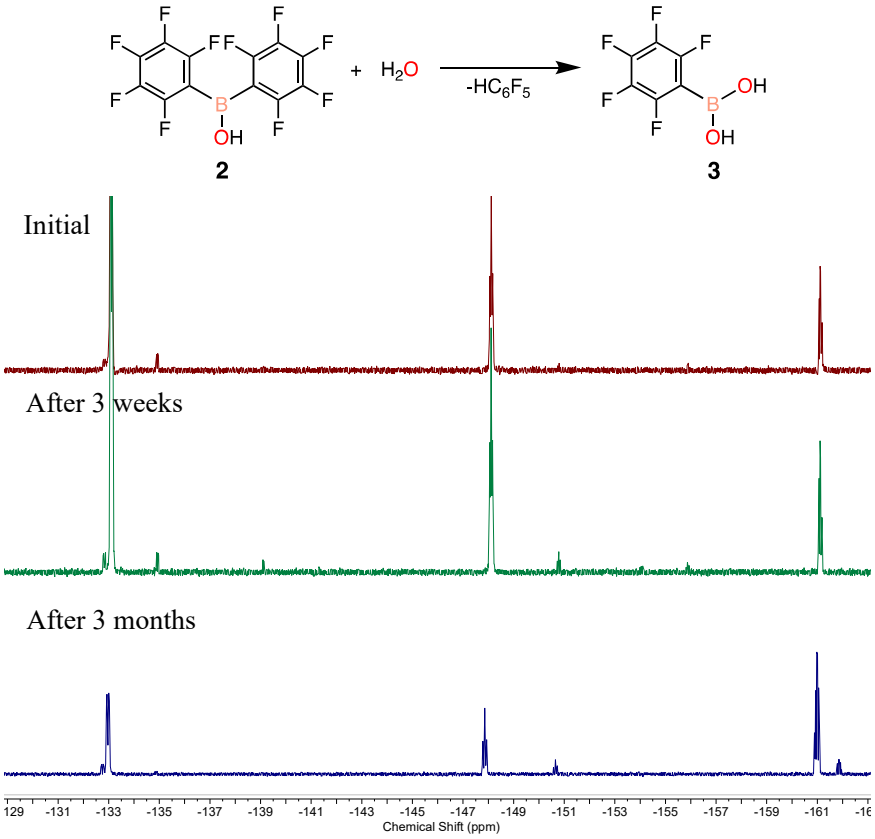

Fig. S19: Stacked $^{19}F\{^{1}H\}$ NMR spectra of borinic acid **2** in the solid state upon exposure to atmosphere in C_6D_6.

Tris(pentafluorophenyl)borane ($B(C_6F_5)_3$):

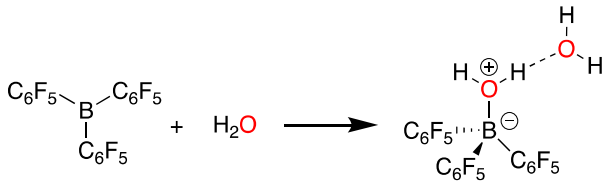

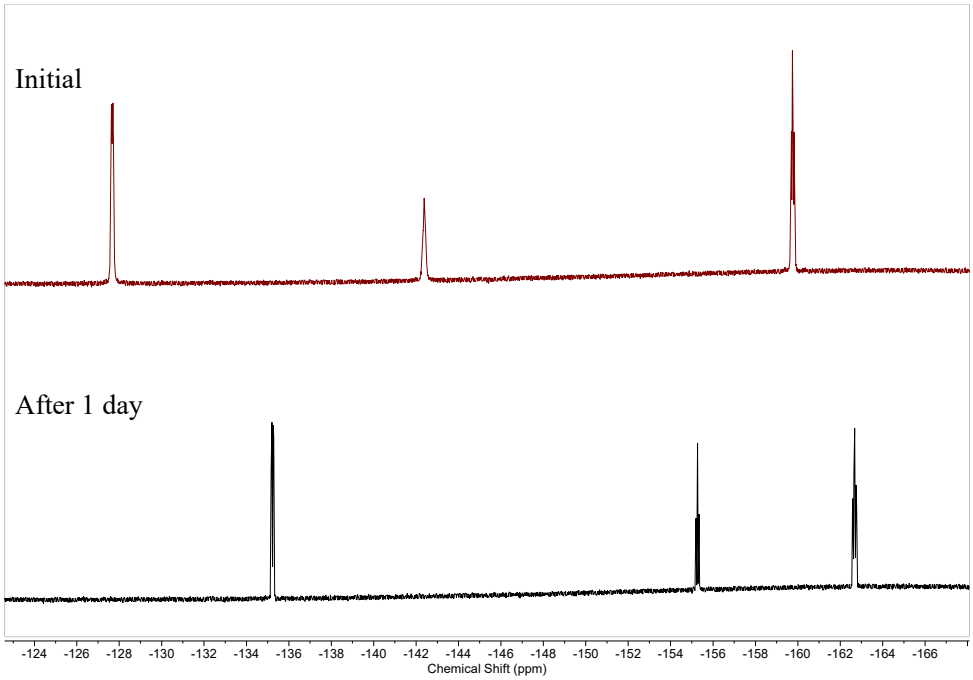

***Fig S20**:* Stacked $^{19}F\{^1H\}$ NMR spectra of $B(C_6F_5)_3$ in the solid state upon exposure to atmosphere in C_6D_6.

Catalytic Experiments

General procedure for hydrosilylation experiments: a mixture containing the corresponding carbonyl substrate (0.100 mmol, 1eq.), triethylsilane (0.110 mmol, 1.1 eq.), mesitylene (0.010 mmol, an internal standard), and respective catalyst (**1**, **2**, or $B(C_6F_5)_3$) (0.005 mmol, 5 mol %) in 0.6 mL deuterated solvent (benzene-d_6, dichloromethane-d_2, chloroform-d, acetonitrile-d_3) was prepared. The mixture was dispensed into sealed NMR tubes, sealed with Parafilm, and allowed to react over time while monitoring *via* quantitative ^{1}H NMR spectroscopy. Control experiments for the hydrosilylation reactions without catalyst were performed in parallel. The reaction was complete upon consumption of starting material or no observable progression in conversion. Chemical shifts of the silyl ether products were consistent with the literature.

Catalytic experiments using Poly(methylhydrosiloxane) (PMHS): Catalytic procedure was followed as outlined previously, using PMHS (1 or 4 eq.) instead of triethylsilane (1.1 eq.). The reaction was monitored *via* quantitative ^{1}H NMR spectroscopy and deemed complete upon disappearance of the aldehydic proton signal. The solution was then treated with 1 eq. of dry methanol to yield the corresponding alcohol displaying chemical shifts consistent with the literature.

Characterization of hydrosilylated products:

((Triethylsiloxy)methyl)benzene[5]:

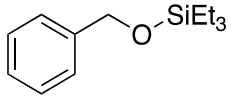

^{1}H NMR (600 MHz, $CDCl_3$) δ: 7.37-7.23 (m, 5H), 4.75 (s, 2H), 0.99 (t, 9H, *J* = 8.0 Hz), 0.67 (q, 6H, *J* = 7.9 Hz).

4-Trifluoromethyl((triethylsiloxy)methyl)benzene[5]:

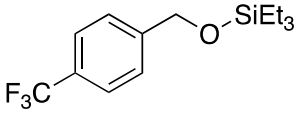

^{1}H NMR (600 MHz, $CDCl_3$) δ: 7.59 (d, 2H, *J* = 8.1 Hz), 7.45 (d, 2H, *J* = 7.9 Hz), 4.79 (s, 2H), 0.98 (t, 9H, *J* = 7.9 Hz), 0.67 (q, 6H, *J* = 7.9 Hz).

4-Bromo((triethylsiloxy)methyl)benzene[5]:

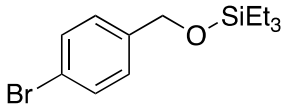

^{1}H NMR (600 MHz, $CDCl_3$) δ: 7.45 (m, 2H), 7.21 (m, 2H), 4.68 (s, 2H), 0.98 (t, 9H, *J* = 7.6 Hz), 0.65 (q, 6H, *J* = 7.9 Hz).

4-Nitro((triethylsiloxy)methyl)benzene[6]:

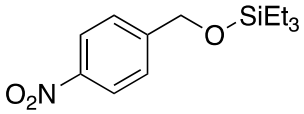

^{1}H NMR (600 MHz, $CDCl_3$) δ: 8.20 (d, 2H, *J* = 8.7 Hz), 7.50 (d, 2H, *J* = 8.4 Hz), 4.83 (s, 2H), 0.99 (t, 9H, *J* = 7.9 Hz), 0.67 (q, 6H, *J* = 8.0 Hz).

4-Methyl((triethylsiloxy)methyl)benzene[7]:

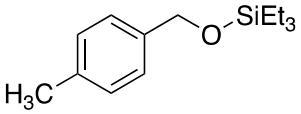

^{1}H NMR (600 MHz, $CDCl_3$) δ: 7.26 (d, 2H, *J* = 7.9 Hz), 7.18 (d, 2H, *J* = 7.8 Hz), 4.73 (s, 2H), 2.37 (s, 3H), 1.01 t, 9H, *J* = 8.0 Hz), 0.68 (q, 6H, *J* = 8.0 Hz).

4-Methoxy((triethylsiloxy)methyl)benzene[5]:

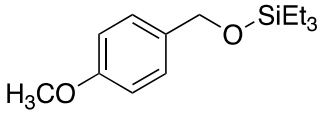

^{1}H NMR (600 MHz, $CDCl_3$) δ: 7.27 (d, 2H, *J* = 8.9 Hz), 6.87 (d, 2H, *J* = 8.7 Hz), 4.87 (s, 2H), 3.80 (s, 3H), 0.98 (t, 9H, *J* = 7.9 Hz), 0.65 (q, 6H, *J* = 8.0 Hz).

4-(((Triethylsilyl)oxy)methyl)-1,1'-biphenyl[7]:

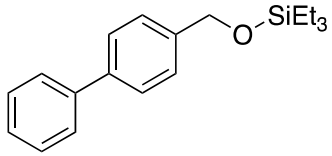

^{1}H NMR (600 MHz, $CDCl_3$) δ: 7.66-7.60 (m, 4H), 7.50-7.44 (m, 4H), 7.36 (m, 1H), 4.80 (s, 2H), 1.02 (t, 9H, *J* = 8.0 Hz), 0.70 (q, 6H, *J* = 8.0 Hz).

1-(((Triethylsilyl)oxy)methyl)naphthalene[8]:

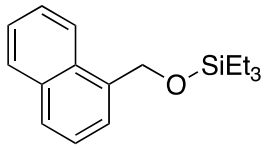

^{1}H NMR (600 MHz, $CDCl_3$) δ: 8.02 (d, 1H, *J* = 8.2 Hz), 7.88 (d, 1H, , *J* = 9.3 Hz), 7.78 (d, 1H, *J* = 8.3 Hz), 7.59-7.48 (m, 4H), 5.22 (s, 2H), 1.01 (t, 9H, *J* = 8.0 Hz), 0.71 (q, 6H, *J* = 8.0 Hz).

((Triethylsilyl)oxy)cyclohexane[5]:

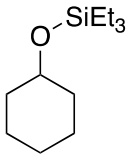

^{1}H NMR (600 MHz, $CDCl_3$) δ: 3.56 (m, 1H), 1.82-1.68 (m, 4H), 1.33-1.09 (m, 5H), 0.95 (t, 9H, *J* = 7.9 Hz), 0.59 (q, 6H, *J* = 8.0 Hz).

(1-((Triethylsilyl)oxy)ethyl)benzene[6]:

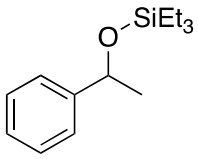

^{1}H NMR (600 MHz, $CDCl_3$) δ: 7.35 (m, 2H), 7.32 (m, 2H), 7.23 (m, 1H), 4.87 (q, 1H, *J* = 6.2 Hz), 1.44 (d, 3H, *J* = 6.5 Hz), 0.92 (t, 9H, *J* = 7.9 Hz), 0.58 (m, 6H).

1,1'-(((Triethylsilyl)oxy)methylene)bisbenzene[6]:

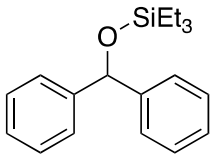

^{1}H NMR (600 MHz, $CDCl_3$) δ: 7.41 (m, 4H), 7.33 (m, 4H), 7.25 (m, 2H), 5.81 (s, 1H), 0.93 (t, 9H, *J* = 8.0 Hz), 0.62 (q, 6H, *J* = 7.8 Hz).

Triethyl(heptyloxy)silane[9]:

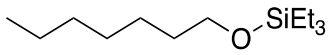

^{1}H NMR (600 MHz, $CDCl_3$) δ: 3.60 (t, 2H, *J* = 6.8 Hz), 1.53 (t, 2H, *J* = 7.3 Hz), 1.39-1.21 (m, 8H), 0.97 (t, 9H, *J* = 6.8 Hz), 0.89 (m, 3H), 0.60 (q, 6H, *J* = 8.0 Hz).

1-Bromo-4-((1E)-3-((trimethylsilyl)oxy)-1-propen-1-yl)benzene:

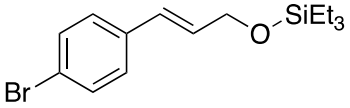

^{1}H NMR (600 MHz, $CDCl_3$) δ: 7.43 (m, 2H), 7.24 (m, 2H), 6.55 (dt, 1H, *J* = 15.8 Hz, 1.8 Hz), 6.29 (dt, 1H, *J* = 15.8 Hz, 5.1 Hz), 4.33 (dd, 2H, *J* = 5.1 Hz, 1.7 Hz), 0.99 (t, 9 H, *J* = 8.1 Hz), 0.67 (q, 6H, *J* = 8.0 Hz). **^{13}C{^{1}H} NMR** (101 MHz, $CDCl_3$) δ: 136.2, 131.7, 130.1, 128.6, 128.1, 127.1, 63.49, 6.9, 4.7. **ESI-MS** $C_{15}H_{22}BrOSi$ (m/z): $[M+H]^+$ calculated: 325.0618; found: 325.0610.

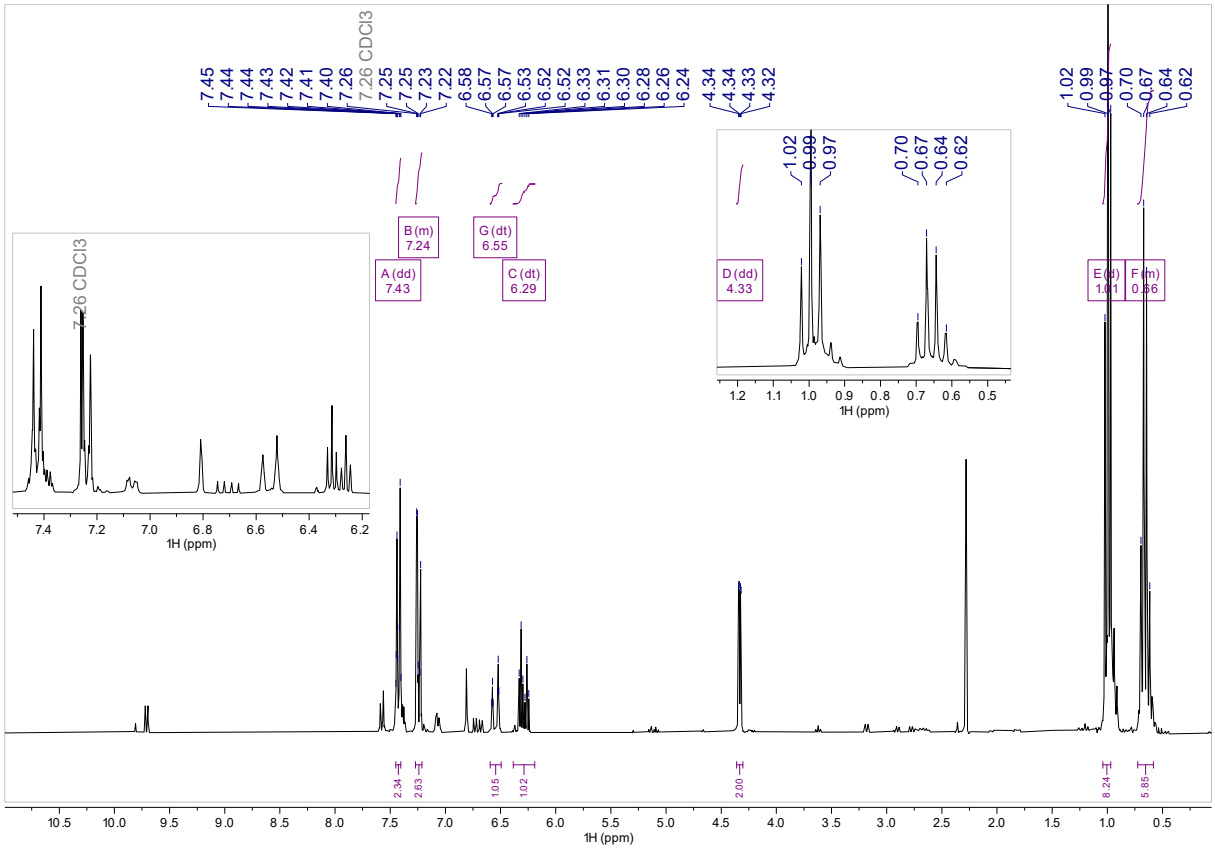

Fig S21: ^{1}H NMR spectrum of 1-Bromo-4-((1E)-3-((trimethylsilyl)oxy)-1-propen-1-yl)benzene in $CDCl_3$.

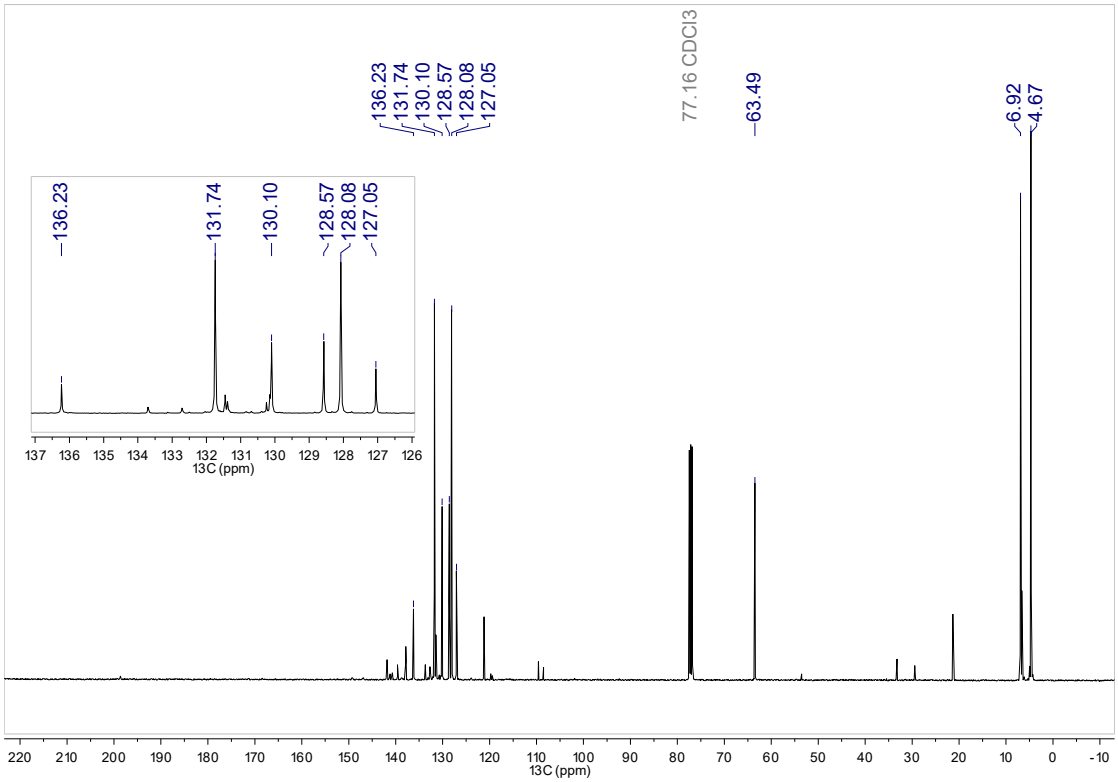

Fig S22: $^{13}C\{^{1}H\}$ NMR spectrum of 1-Bromo-4-((1E)-3-((trimethylsilyl)oxy)-1-propen-1-yl)benzene in $CDCl_3$.

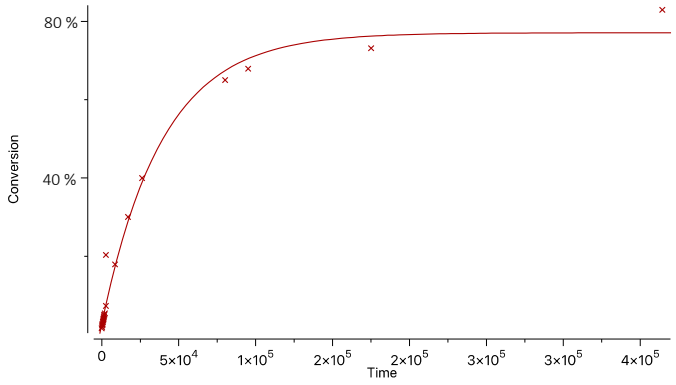

Fig S23: Plot of conversion vs time of the hydrosilylation of benzaldehyde using triethylsilane and 2.

Test Reactions with Triethylsilane and 2

Bis(pentafluorophenyl)borinic acid (18.1 mg, 0.05 mmol) was dissolved in 0.6 mL of $CDCl_3$ and added to an NMR tube. Triethylsilane (7.99 μL, 0.05 mmol, 1 eq.) was added to the solution and the resulting silyl ether product was characterized by NMR spectroscopy.

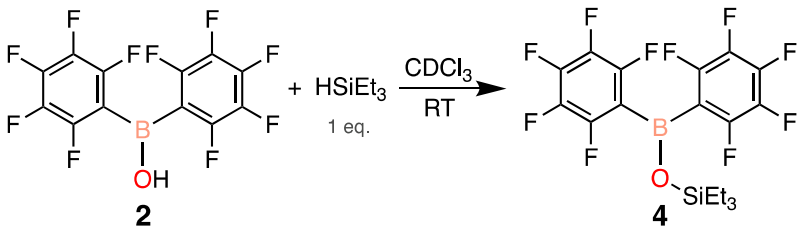

^{1}H NMR (400 MHz, $CDCl_3$) δ: 0.93 (t, 9H, *J* = 7.9 Hz), 0.67 (q, 6H, *J* = 8.0 Hz).

^{19}F NMR (376 MHz, $CDCl_3$) δ: -132.6 (m, 2F), -149.4 (tt, 1F, *J* = 19.9 Hz, *J* = 3.7Hz), -161.1 (m, 2F).

^{11}B{^{1}H} NMR (128 MHz, $CDCl_3$) δ: 38.3 (br).

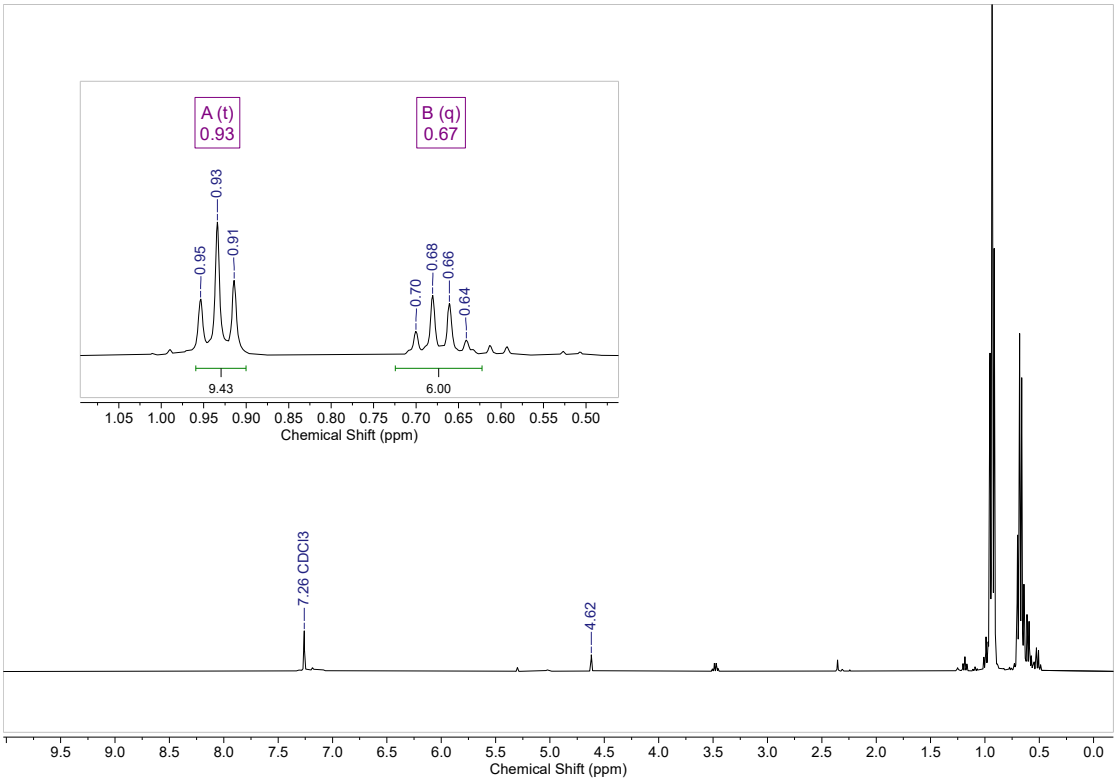

Fig S24: ^{1}H NMR spectrum of silyl ether **4** in $CDCl_3$.

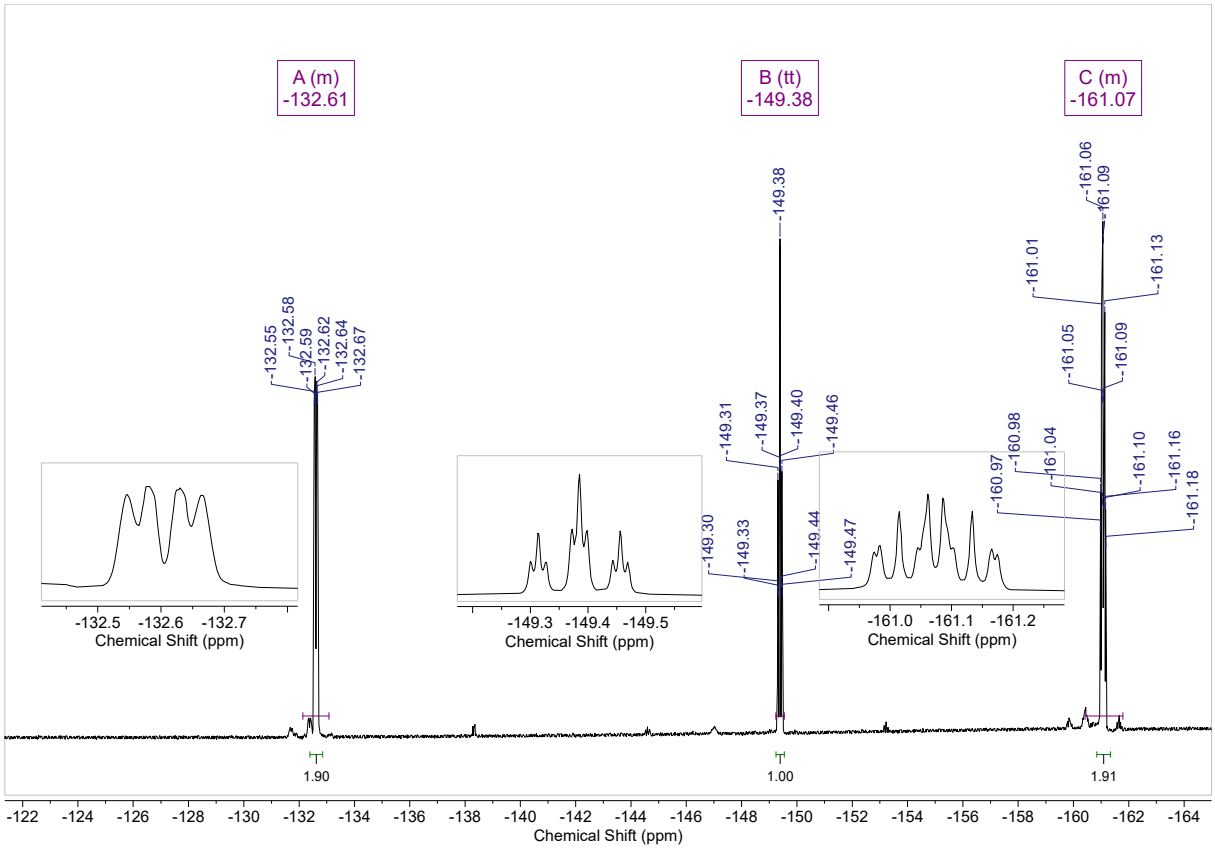

***Fig S25**:* ^{19}F NMR spectrum of silyl ether **3** in $CDCl_3$.

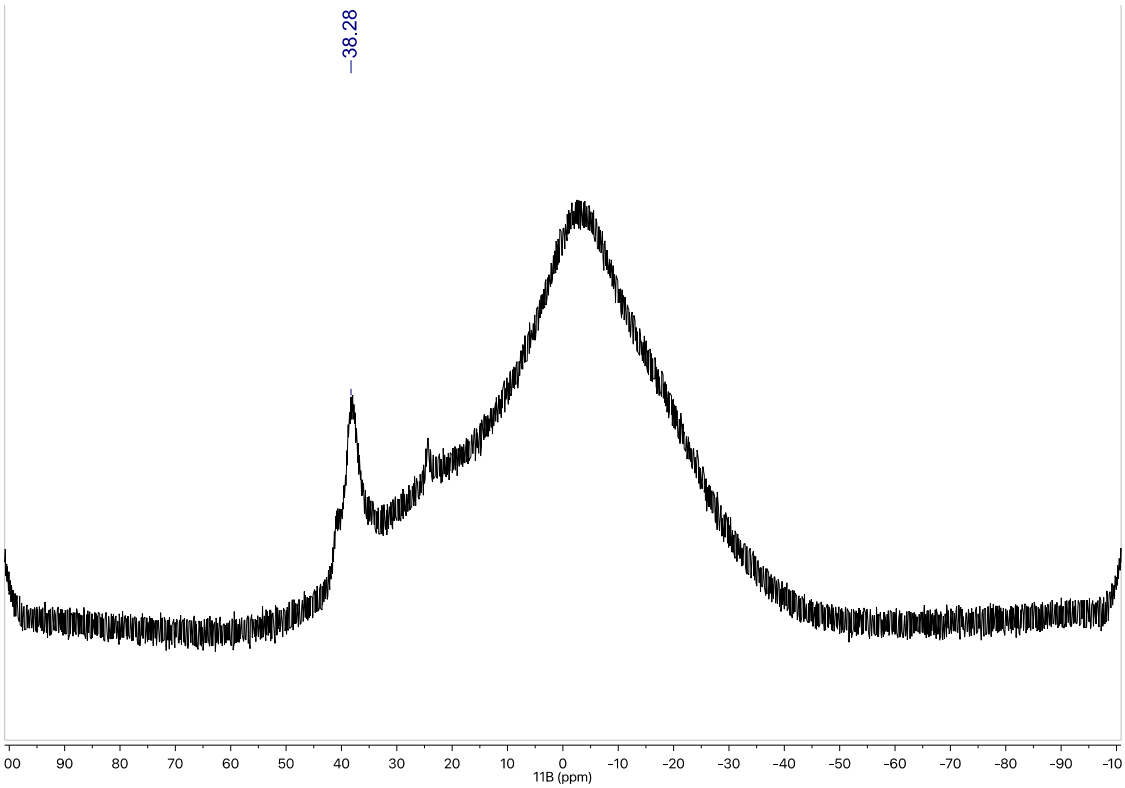

***Fig S26**:* $^{11}B\{^{1}H\}$ NMR spectrum of silyl ether **3** in $CDCl_3$.

Computational Details

Fluoride ion affinity (FIA) calculations were completed using Gaussian 16 suite of quantum chemistry programs.[10] The geometry optimizations of all molecules were carried out using B3LYP[11,12] level of theory and def2-QZVPP[13,14] basis sets with conductor-like polarizable continuum (CPCM) dichloromethane solvation model.[15] The optimized structures were subjected to normal mode frequency calculations using the same computational methods. The results of the frequency analysis contained zero imaginary frequencies, showing that these structures converge to a stationary point on the potential energy surface. Thermochemical parameters, such as enthalpies, were obtained from the frequency calculations and used to determine the FIA values following the protocol as defined by Erdmann *et al*.[16]

Optimized Coordinates

$(C_6F_5)_2BOH$

B	-0.02823300	1.36287500	0.17968700
C	-1.38929600	0.59077000	-0.01721100
C	-1.47290500	-0.64936200	-0.65305900
F	-0.38088700	-1.22852700	-1.16084600
C	-2.66608800	-1.33561700	-0.81248100
F	-2.69700100	-2.51367300	-1.43079400
C	-3.84151000	-0.78375200	-0.32517900
F	-4.99065000	-1.42898800	-0.46958300
C	-3.81234500	0.45185500	0.30606800
F	-4.93915700	0.98914900	0.76867800
C	-2.60259100	1.10870400	0.43683800
F	-2.63465000	2.31086900	1.04732700
C	1.36921600	0.63897700	0.15573000
C	2.43238400	1.12484100	-0.59777000
F	2.26721000	2.19943800	-1.37751500

C	3.67659200	0.51370600	-0.60938000
F	4.66898600	0.99580500	-1.35718400
C	3.88595100	-0.61611200	0.16784800
F	5.07520000	-1.20897200	0.17361600
C	2.85182100	-1.12723400	0.93971000
F	3.05566200	-2.20890700	1.69148300
C	1.62001400	-0.49727500	0.91475800
F	0.64225200	-1.01663200	1.67528100
O	0.00964400	2.69204000	0.39711100
H	-0.84612400	3.12622700	0.44526300

$[(C_6F_5)_2BF(OH)]^-$

B	-0.00024700	1.66326600	-0.10218700
C	-1.36446800	0.67055800	-0.14822900
C	-1.40547500	-0.44408000	-0.97531200
F	-0.34468100	-0.76148200	-1.74489900
C	-2.49688300	-1.29368100	-1.07504900
F	-2.47530800	-2.36538700	-1.88761300
C	-3.63205100	-1.03098700	-0.32761600
F	-4.70396400	-1.83628600	-0.41041100
C	-3.65018500	0.07824300	0.49790800
F	-4.75528600	0.35083300	1.21605800
C	-2.53062000	0.89621000	0.56470200
F	-2.65420600	1.97177600	1.38084500
C	1.35926100	0.71914600	0.05283100
C	2.47015700	0.78300700	-0.77571700
F	2.51528000	1.62192600	-1.82450600
C	3.60379300	0.00103900	-0.58811700
F	4.65854100	0.09981400	-1.41899800

C	3.65597600	-0.89039100	0.46774600
F	4.74558000	-1.65290700	0.66269200
C	2.57217900	-0.98536700	1.32308700
F	2.61493400	-1.85024900	2.35372000
C	1.46221600	-0.18512600	1.10058900
F	0.44257400	-0.33820400	1.97035300
O	0.03932700	2.56180300	1.02128300
H	-0.78507600	3.03513200	1.12668600
F	-0.02032100	2.34268700	-1.35134700

COF_2

C	0.00000000	0.00000000	0.14098000
O	0.00000000	0.00000000	1.31297500
F	0.00000000	1.06423200	-0.63053800
F	0.00000000	-1.06423200	-0.63053800

$[COF_3]^-$

C	0.00100000	-0.00128100	0.18632000
O	0.00785200	-0.00884300	1.40443400
F	0.95435000	-0.83702500	-0.46806100
F	0.24657300	1.25143200	-0.45111000
F	-1.20857000	-0.40569300	-0.45342800

Compound	**Enthalpy (gas phase) (Hartree)**	**Enthalpy (DCM) (Hartree)**
$(C_6F_5)_2BOH$	-1557.014400	-1557.022388
$[(C_6F_5)_2BF(OH)]^-$	-1657.044017	-1657.103554
COF_2	-313.159845	-313.162501
$[COF_3]^-$	-413.137909	-413.223151

References

1. Bentley, J. N.; Pradhan, E.; Zeng, T.; Caputo, C. B. *Dalton Trans.* **2020**, *49*, 16054–16058.
2. Bentley, J. N.; Simoes, S. A.; Pradhan, E.; Zeng, T.; Caputo, C. B. *Org. Biomol. Chem.* **2021**, *19*, 4796–4802.
3. Zhang, J.; Park, S.; Chang, S. *Angew. Chem. Int. Ed.* **2017**, *56*, 13757–13761.
4. Mayer, U.; Gutmann, V.; Gerger, W. *Monatshefte Für Chem.* **1975**, *106*, 1235–1257.
5. Chan, Y.; Bai, Y.; Chen, W.; Chen, H.; Li, C.; Wu, Y.; Tseng, M.; Yap, G. P. A.; Zhao, L.; Chen, H.; Ong, T. *Angew. Chem. Int. Ed.* **2021**, *60*, 19949–19956.
6. Chen, P.-H.; Hsu, C.-P.; Tseng, H.-C.; Liu, Y.-H.; Chiu, C.-W. *Chem. Commun.* **2021**, *57*, 13732–13735.
7. Sarkar, N.; Sahoo, R. K.; Mukhopadhyay, S.; Nembenna, S. *Eur. J. Inorg. Chem.* **2022**, *2022*, e202101030.
8. Bajracharya, G. B.; Nogami, T.; Jin, T.; Matsuda, K.; Gevorgyan, V.; Yamamoto, Y. *Synthesis* **2004**, *2*, 308–311.
9. Field, L. D.; Messerle, B. A.; Rehr, M.; Soler, L. P.; Hambley, T. W. *Organometallics* **2003**, *22*, 2387–2395.
10. Gaussian 16, Revision C.01, M. J. Frisch, G. W. Trucks, H. B. Schlegel, G. E. Scuseria, M. A. Robb, J. R. Cheeseman, G. Scalmani, V. Barone, G. A. Petersson, H. Nakatsuji, X. Li, M. Caricato, A. V. Marenich, J. Bloino, B. G. Janesko, R. Gomperts, B. Mennucci, H. P. Hratchian, J. V. Ortiz, A. F. Izmaylov, J. L. Sonnenberg, D. Williams-Young, F. Ding, F. Lipparini, F. Egidi, J. Goings, B. Peng, A. Petrone, T. Henderson, D. Ranasinghe, V. G. Zakrzewski, J. Gao, N. Rega, G. Zheng, W. Liang, M. Hada, M. Ehara, K. Toyota, R. Fukuda, J. Hasegawa, M. Ishida, T. Nakajima, Y. Honda, O. Kitao, H. Nakai, T. Vreven, K. Throssell, J. A. Montgomery, Jr., J. E. Peralta, F. Ogliaro, M. J. Bearpark, J. J. Heyd, E. N. Brothers, K. N. Kudin, V. N. Staroverov, T. A. Keith, R. Kobayashi, J. Normand, K. Raghavachari, A. P. Rendell, J. C. Burant, S. S. Iyengar, J. Tomasi, M. Cossi, J. M. Millam, M. Klene, C. Adamo, R. Cammi, J. W. Ochterski, R. L. Martin, K. Morokuma, O. Farkas, J. B. Foresman, and D. J. Fox, Gaussian, Inc., Wallingford CT, 2016.
11. Lee, C.; Yang, W.; Parr, R. G. *Phys. Rev. B* **1988**, *37*, 785–789.
12. Becke, A. D. *J. Chem. Phys.* **1993**, *98*, 5648–5652.
13. Weigend, F.; Ahlrichs, R. *Phys. Chem. Chem. Phys.* **2005**, *7*, 3297.
14. Weigend, F. *Phys. Chem. Chem. Phys.* **2006**, *8*, 1057.
15. Foresman, J. B.; Keith, T. A.; Wiberg, K. B.; Snoonian, J.; Frisch, M. J. *J. Phys. Chem.* **1996**, *100*, 16098–16104.
16. Erdmann, P.; Leitner, J.; Schwarz, J.; Greb, L. *ChemPhysChem* **2020**, *21*, 987–994.